constants
A_{i0} = pre-exponential factors of main reaction rate constant
C_p = specific heat of reaction mixture
C_1 = cost of separation of reactant from product
C_2 = cost of separation of byproduct from product
C_3 = cost of reactant
E = activation energy of fouling reaction rate constant
E_i = activation energies of main reaction rate constants
f_i' = rate of the i^{th} chemical reaction
G, G_1, G_2 = integrands of objective functional
g_k' = rate of the k^{th} fouling reaction
H, H_1, H_2 = Hamiltonians
ΔH_i = heat of reaction of the i^{th} chemical reaction
h_i = blending function
I = objective functional
$J_i = \left(\frac{-\Delta H_i}{C_p}\right)\left(\frac{R}{E_1}\right)$
L' = total reactor residence time
P = pressure
$p = E_1/E$
$p_1 = E_2/E_1$
q_0' = reference feed rate
$\mathbf{q}_k'$ = feed rate vector to k^{th} bed
$\mathbf{q}_k$ = dimensionless feed rate vector to k^{th} bed = $\mathbf{q}_k'/q_0'$
T = temperature
t' = time
$t = t'/\theta$
$\mathbf{u}_k$ = control variable vector in the k^{th} bed
V = total reactor volume
$w(z)$ = initial catalyst activity along the reactor length
x, y = state variables
z' = residence time in the reactor
z = dimensionless spatial coordinate

Greek Letters

α_k^- = spatial coordinate of end of $(k-1)^{st}$ bed
α_k^+ = spatial coordinate at beginning of k^{th} bed
$\beta_1 = A_{10} \cdot L$
$\beta_2 = A_{20} \cdot L$
$\hat{\beta}_1 = A_{10}V/q_0'$
$\hat{\beta}_2 = A_{20}V/q_0'$
ϵ = scalar constant
θ = total on-stream time
$\lambda_i\mu_i$ = adjoint variables
ξ_i = extent of the i^{th} reaction, or concentration of i^{th} species
$\rho = A_0\theta$
$\tau = RT/E_1$
Ψ_k = instantaneous catalyst activity for the k^{th} catalytic agent

LITERATURE CITED

1. Ogunye, A. F., and W. H. Ray, *AIChE J.*, **17**, 43 (1971).
2. Crowe, C. M., paper presented at AIChE Washington Meeting (Nov. 1969).
3. Aris, Rutherford, "Elementary Chemical Reactor Analysis," p. 65, Prentice-Hall, Englewood Cliffs, N. J. (1968).
4. Johansen, D. E., "Advan. Control Systems," **4**, 279 (1966).
5. Ogunye, A. F., Ph.D. thesis, Univ. Waterloo, Canada (1969).

Manuscript received August 20, 1969; revision received January 1, 1970; paper accepted January 19, 1970.

Diffusion and Reaction in Ideal Multicomponent Systems:

I. Tubular Reactor near Equilibrium

R. L. SOLOMON and J. L. HUDSON

University of Illinois, Urbana, Illinois

Diffusion and either surface or gas-phase reaction in a ternary ideal gas mixture in steady fully developed laminar flow in a tube is considered. The linearized equations valid near equilibrium and under isothermal conditions are solved. Concentration profiles predicted using a multicomponent diffusivity matrix are compared to those predicted using more approximate diffusivities. Local overshoots past equilibrium occur, but oscillations (with axial position) are not possible. A simplified diffusivity expression is found which predicts cup-mixing mole fractions in good agreement with those predicted using the multicomponent diffusivities.

In a multicomponent mixture the diffusional flux of each component depends on the spatial variation of the concentration of all the species. If the fluxes depend linearly on the mole fraction gradients according to an expression of the form

$$J_i^* = -c \sum_{j=1}^{N} D_{ij}^* \nabla x_j \qquad (1)$$

and if no chemical reaction occurs, the species mass balances can be uncoupled; the solutions of the equations governing the multicomponent system can then be found in terms of solutions of analogous binary problems (*6, 7, 27, 29, 30*).

If a chemical reaction occurs the species mass balances can not, in general, be uncoupled (*31*). Interesting and important effects due to the coupling in diffusion and reaction can occur in multicomponent systems. Toor (*31*) considered transient diffusion and gas-phase reaction in a one-dimensional nonflow multicomponent system. The linearized equations were solved by separation of variables. Toor showed that the eigenvalues for an ideal system near

R. L. Solomon is at Manchester University, Manchester, England.

equilibrium are always real and positive so that the system is stable and the time behavior is nonoscillatory. Overshoots in time near equilibrium are however possible. Transient diffusion and surface reaction in a one-dimensional system without flow has also been considered (*12*).

In this work multicomponent diffusion and chemical reaction in a tubular reactor are considered. It is assumed that the flow is fully developed, laminar, and steady. The fluid is an ideal gas near chemical equilibrium and the reaction rate expressions are linearized about their equilibrium values. The mixture is isothermal. A diffusional flux expression of the form (1) is used where the diffusivities are assumed to be constant and equal to their values at equilibrium. Representative reactions are considered and values for the rate constants are taken from the literature. Both gas-phase and surface reactions are treated. The concentration profiles and reaction rates predicted using the multicomponent diffusion flux expression (1) are compared to those predicted using a flux expression of the form

$$J_i^* = -c\ D_i^*\ \nabla x_i \qquad (2)$$

where the D_i are not equal. In addition, the predicted concentration profiles and reaction rates are compared to those obtained using (2) with all D_i equal. The results are limited to ternary systems. Both irreversible and reversible reactions are considered.

This work on ternary diffusion and reaction in a tubular reactor is an extension of previous work on a single irreversible reaction in dilute systems. Fluid-phase reactions (*10, 14, 25, 32*), surface reactions (*2, 13, 21, 22, 25*), and simultaneous fluid-phase and surface reactions (*25*) have been treated.

Studies of coupled reactions are limited, although fluid-phase (*34*) and surface reactions (*11, 15*) have been considered in a tubular reactor using a diffusional flux law of the form (2); in the case of consecutive reactions with uncoupled diffusion the mass balances are uncoupled in the sense that they can be solved consecutively. Coupled reactions in a flow system have also been considered using the flux law (2) with equal diffusivities (*16, 17*); when the diffusion coefficients are equal the mass balance equations can be uncoupled by a transformation.

ANALYSIS

Consider a ternary isothermal ideal gas in a tubular reactor. The three species take part in a chemical reaction for which there is no volume change. It is assumed that the flow is laminar and steady and that axial diffusion may be neglected. It is further assumed that the mixture is near chemical equilibrium such that the reaction rate expressions may be linearized around their equilibrium values and that the multicomponent diffusivities and the viscosity may be taken as constant and equal to their values at equilibrium. Under these conditions the dimensionless mass balances are

$$\{1-\eta^2\}\frac{\partial(y)}{\partial z} = [D]\,\nabla_\eta^2\,(y) + [K]\,(y) \qquad (3)$$

where

$$\nabla_\eta^2 = \frac{1}{\eta}\frac{\partial}{\partial\eta}\eta\frac{\partial}{\partial\eta}$$

with boundary conditions

$$(y) = (y^0) \qquad z = 0 \qquad (4)$$

$$[D]\frac{\partial(y)}{\partial\eta} + [F]\,(y) = 0 \qquad \eta = 1 \qquad (5)$$

and in addition the mole fractions are symmetric about $\eta = 0$. The vector (y) is the deviation of the mole fractions away from their equilibrium values. For a ternary system the vector (y) has two components; the third component has been eliminated using the fact that the sum of the mole fractions is one. In the work that follows the component eliminated will always be that which has the largest equilibrium concentration. The dimensionless linearized gas-phase and surface reaction rate constant matrices $[K]$ and $[F]$ and the diffusion matrix $[D]$ are defined by

$$[K] = [K^*]\ R^2/D_R$$
$$[F] = [F^*]\ R/D_R$$
$$[D] = [D^*]/D_R$$

In the examples considered, one of the matrices $[K]$ or $[F]$ is always zero so that the reactions occur only on the tube surface or in the gas phase; however the analysis does hold for both $[K]$ and $[F]$ nonzero.

The elements of the diffusivity matrix D will be chosen in one of three ways. Multicomponent diffusion coefficients are first considered and are designated $[D]_{MC}$. The multicomponent diffusion coefficients can be determined from the binary diffusivities $\mathcal{D}_{12}$, $\mathcal{D}_{13}$, $\mathcal{D}_{23}$ and the equilibrium concentrations for an ideal gas (*5, 9*). In general no element of $[D]_{MC}$ is zero. There are three independent coefficients for a ternary system. The binary diffusivities are estimated from the Wilke-Lee correlation (*19, 33*). The second manner of choosing $[D]$ is to use binary diffusivities. Equations (3) are written for the two least concentrated species (say 1 and 2). The diffusivities of species 1 and 2 are then $\mathcal{D}_{13}$ and $\mathcal{D}_{23}$, respectively. The matrix $[D]$ is thus diagonal and is designated $[D]_B$. The matrices $[D]_{MC}$ and $[D]_B$ become equal as the mole fractions x_1 and x_2 approach zero. The third diffusivity matrix considered is formulated using effective diffusivities for components 1 and 2 where these effective diffusivities are obtained from (3):

$$D_i^* = \frac{1-(x_i)_e}{\sum_{\substack{j=1\\ j\neq i}}^{N}\frac{(x_j)_e}{\mathcal{D}_{ij}}} \qquad i = 1, 2 \qquad (7)$$

The dimensionless matrix with elements D_i^*/D_R is designated $[D]_E$. Although both $[D]_B$ and $[D]_E$ are diagonal, the elements of a diagonal are, in general, not equal. Thus the mathematics involved in using $[D]_B$ or $[D]_E$ is no simpler than that involved in using $[D]_{MC}$, since in no case can Equations (3) be uncoupled. The problem is greatly simplified if a diffusivity matrix can be used which is a constant times the identity matrix, that is, all the diffusivities are equal; in this case Equations (3) can be uncoupled if either only gas-phase or only surface reactions take place. Such a diffusivity matrix is determined below and is designated $\bar{D}\,[I]$.

Equations (3) with boundary conditions (4) and (5) are solved by the Galerkin method. It is convenient to first uncouple the boundary condition (5); of course if no surface reaction occurs (5) is already uncoupled and this step is unnecessary. The matrix $[\bar{D}]$ can always be inverted (*6, 29, 30*). The modal matrix $[T]$ of $[\bar{D}]^{-1}\,[F]$ is thus found and (5) becomes

$$\frac{\partial(\psi)}{\partial\eta} + [\mu]\,(\psi) = 0 \qquad \eta = 1 \qquad (8)$$

where

$$(\psi) = [T]^{-1}\,(y) \qquad (9)$$

$$[T]^{-1}\,[D]^{-1}[F]\,[T] = [\mu] \qquad (10)$$

where $[\mu]$ is diagonal and has elements μ_1 and μ_2. Equation (3) with (4) transforms to

$$\{1-\eta^2\}\frac{\partial(\psi)}{\partial z} = [H]\,\nabla_\eta^2\,(\psi) + [L]\,(\psi) \qquad (11)$$

$$(\psi) = (\psi^0) = [T]^{-1}\,(y^0) \qquad z = 0 \qquad (12)$$

where

$$[H] = [T]^{-1}\,[D]\,[T] \qquad (13a)$$

$$[L] = [T]^{-1}\,[K]\,[T] \qquad (13b)$$

Equation (11) with (8) and (12) is solved by the Galerkin method. (ψ) is expanded in a set of trial functions.

$$\psi_i = \sum_{j=1}^{M} a_{ij}(z)\;\varphi_{ij}(\eta) \qquad (14)$$

where $\varphi_{ij}(\eta) = \cos \alpha_{ij}\,\eta$. The α_{ij} are chosen to be roots of

$$\alpha_{ij} = \mu_i \cot \alpha_{ij} \qquad \begin{matrix} j = 1 \ldots M \\ i = 1, N-1 \end{matrix} \qquad (15)$$

in which case boundary condition (8) is satisfied exactly. The set (14) is complete for $M \to \infty$. The series is truncated after M terms and the error is made orthogonal to the i^{th} trial function weighted by η. Thus the mass balances for components 1 and 2 are multiplied by $\eta\varphi_{ij}\,d\eta$ and $\eta\varphi_{2j}\,d\eta$, respectively, and integrated from $\eta = 0$ to $\eta = 1$. This yields a set of $2M$ ordinary differential equations:

$$[Z]\frac{d(a)}{dz} = [W]\,(a) \qquad (16)$$

where (a) is a vector of $2M$ elements

$$(a) = \begin{bmatrix} a_{11} \\ a_{12} \\ \cdot \\ \cdot \\ \cdot \\ a_{1M} \\ a_{21} \\ \cdot \\ \cdot \\ \cdot \\ a_{2M} \end{bmatrix} \qquad (16a)$$

The matrices $[Z]$ and $[W]$ are $2M \times 2M$. $[Z]$ is partitioned into four $M \times M$ submatrices

$$[Z] = \begin{bmatrix} Z_{11}{}^P & Z_{12}{}^P \\ Z_{21}{}^P & Z_{22}{}^P \end{bmatrix} \qquad (17)$$

where each element of $[Z_{12}{}^P]$ and $[Z_{21}{}^P]$ is zero and

$$(Z_{11}{}^P)_{ij} = \int_0^1 \varphi_{1i}\,\varphi_{1j}\,\eta\{1-\eta^2\}\,d\eta \qquad (18a)$$

$$(Z_{22}{}^P)_{ij} = \int_0^1 \varphi_{2i}\,\varphi_{2j}\,\eta\{1-\eta^2\}\,d\eta \qquad (18b)$$

The matrix $[Z]$ is symmetric.

$[W]$ is the sum of $[A]$ and $[B]$, and $[A]$ and $[B]$ are each partitioned into four $M \times M$ matrices as in Equation (17). Denote the mn^{th} element of the ij^{th} submatrix as A_{imjn} and B_{imjn}. Then

$$A_{imjn} = H_{ij}\int_0^1 \varphi_{im}\frac{d}{d\eta}\,\eta\,\frac{d}{d\eta}\,\varphi_{jn}\,d\eta \qquad (19a)$$

$$B_{imjn} = L_{ij}\int_0^1 \varphi_{im}\,\varphi_{jn}\,\eta\,d\eta \qquad (19b)$$

The matrix $[W]$ is not symmetric.

The solution to (16) is

$$(a) = \sum_{i=1}^{2M} \omega_i\,(C)_i\,e^{\lambda_i z} = [C]\,(S) \qquad (20)$$

where the λ_i are the $2M$ eigenvalues of $[Z]^{-1}\,[W]$ and $[C]$ is the matrix whose columns are the eigenvectors $(C)_i$. The i^{th} element of (S) is $S_i = \omega_i\,e^{\lambda_i z}$.

The coefficients ω_i are found from the boundary condition at $z = 0$:

$$\psi_i{}^0 = \sum_{j=1}^{M} a_{ij}(0)\varphi_{ij} \qquad i = 1, 2 \qquad (21)$$

Multiplying Equations (21) by $\eta\varphi_{1j}\,d\eta$ and $\eta\varphi_{2j}\,d\eta$ and integrating from $\eta = 0$ to $\eta = 1$ yields

$$(Q) = [P]\;(a(0)) \qquad (22)$$

where

$$(Q) = \begin{bmatrix} \psi_1{}^0\int_0^1 \varphi_{11}\,\eta\,d\eta \\ \cdot \\ \cdot \\ \cdot \\ \psi_2{}^0\int_0^1 \varphi_{2M}\,\eta\,d\eta \end{bmatrix} \qquad (23)$$

$[P]$ is a $2M \times 2M$ matrix which is partitioned into four $M \times M$ matrices of which $[P_{12}{}^P]$ and $[P_{21}{}^P]$ are null, while

$$(P_{11}{}^P)_{ij} = \int_0^1 \varphi_{1i}\,\varphi_{1j}\,\eta\,d\eta \qquad (24a)$$

$$(P_{22}{}^P)_{ij} = \int_0^1 \varphi_{2i}\,\varphi_{2j}\,\eta\,d\eta \qquad (24b)$$

$$i, j = 1, \ldots M$$

Since

$$(a(0)) = [C]\,(\omega),$$

$$(\omega) = \{\,[P]\,[C]\,\}^{-1}\,(Q) \qquad (25)$$

The solution for the concentration profiles is now complete. It will be of interest to have an expression for the cup-mixing mole fraction ($\hat{y}$) This is

$$(\hat{y}) = [T]\;(\hat{\psi}) \qquad (26a)$$

where

$$\hat{\psi}_i = 4\sum_{j=1}^{M} a_{ij}(z)\int_0^1 \varphi_{ij}\,\eta\{1-\eta^2\}\,d\eta \qquad (26b)$$

$$i = 1, 2$$

By integration of (3) over the tube cross section it can be shown that the $\hat{y}_i$ are stoichiometric. For example, for the reaction $A + B \rightleftarrows 2C$, $\hat{y}_A = \hat{y}_B = -\frac{1}{2}\,\hat{y}_C$. This can also be seen from a mass balance around a volume from the reactor inlet to a point a finite distance downstream; since the $\hat{y}_i$ are stoichiometric at the inlet and axial diffusion has been neglected, the $\hat{y}_i$ must be stoichiometric at every downstream position.

The transformation (9) is only necessary if $[F]$ is nonzero and the boundary conditions at $\eta = 1$ are coupled. If no surface reaction occurs Equations (3) with (4) and (5) are solved by the Galerkin method. The roots α_{ij} are then $(j-1)\pi$; $j = 1, 2, \ldots M$; $i = 1, 2$.

The numerical calculations were carried out on an IBM 7094. The roots of (15) were obtained by the Newton-Raphson method (23). All the integrals were evaluated analytically. The eigenvalues of $[Z]^{-1}\,[W]$ were found

by the method due to Parlett (*18, 24*). The eigenvectors were found by inverse iteration. Up to a 20-term expansion was used which gave 40 eigenvalues, 20 to 25 of which had at least three-place accuracy. In most cases 9- to 15-term expansions for gas-phase reaction and 12- to 15-term expansions for surface reactions yielded three- to four-figure accuracy in mole fractions for $z \geq 0.1$. The solutions agreed well with previous results for limiting cases (*25, 34*).

RESULTS

Representative calculations will be presented; further results can be found in reference *24*.

Consider first the gas-phase reaction $H_2 + I_2 \rightleftarrows 2HI$. The reaction rate data of Bodenstein (*4*) and of Graven (*8*) are used. These rate expressions have been recently modified to take into account a trimolecular free radical effect (*28*); this effect is greatest at high temperatures. However, the reaction rate constant matrices obtained by linearizing the two rate expressions around equilibrium differ only by a constant factor. The two rate expressions thus lead to similar results; the results can be made identical by considering a slightly different tube radius in the two cases. The older rate expressions are thus used in this study.

As a first example consider $T = 978°K.$, $P = 0.9$ atm., and an equimolar equilibrium state (13.5% H_2, 13.5% I_2, and 73% HI). The dimensionless multicomponent and binary diffusivity matrices are

$$[D]_{MC} = \begin{bmatrix} 0.956 & 0.0029 \\ -0.133 & 0.0951 \end{bmatrix} \qquad (27)$$

and

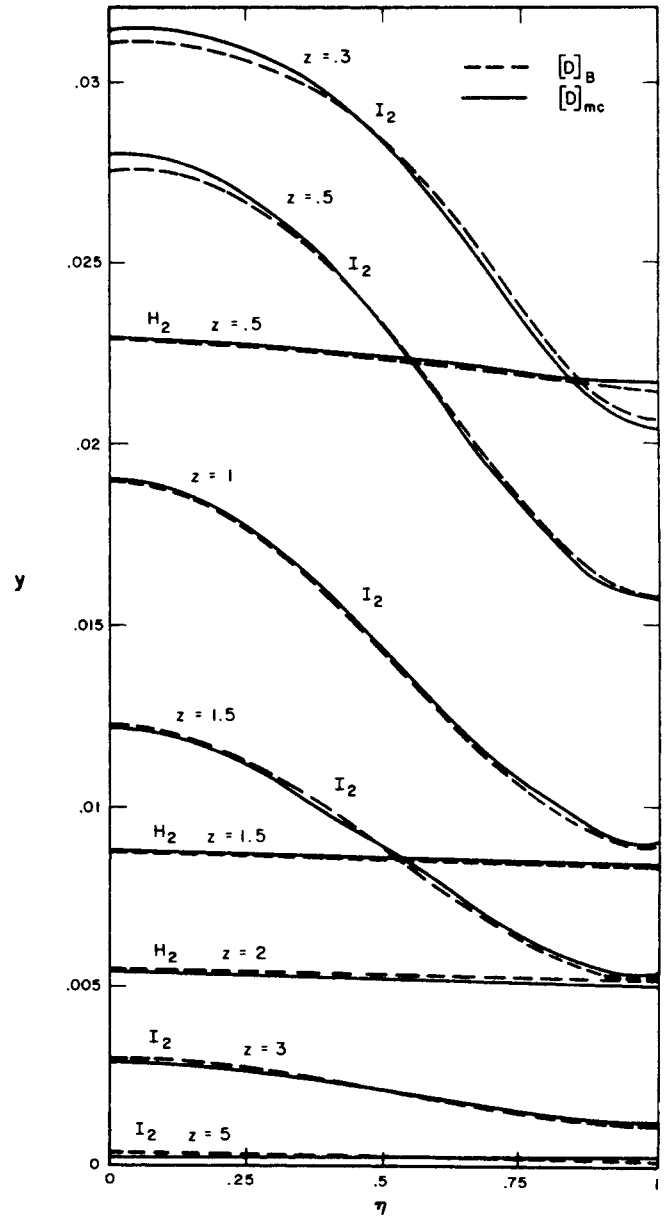

Fig. 1. Radial profiles of mole fraction in the tubular reactor near equilibrium; H_2, I_2; $P = 0.9$ atm., $T = 978°K.$; stoichiometric equilibrium ($H_2 + I_2 \rightleftarrows 2HI$).

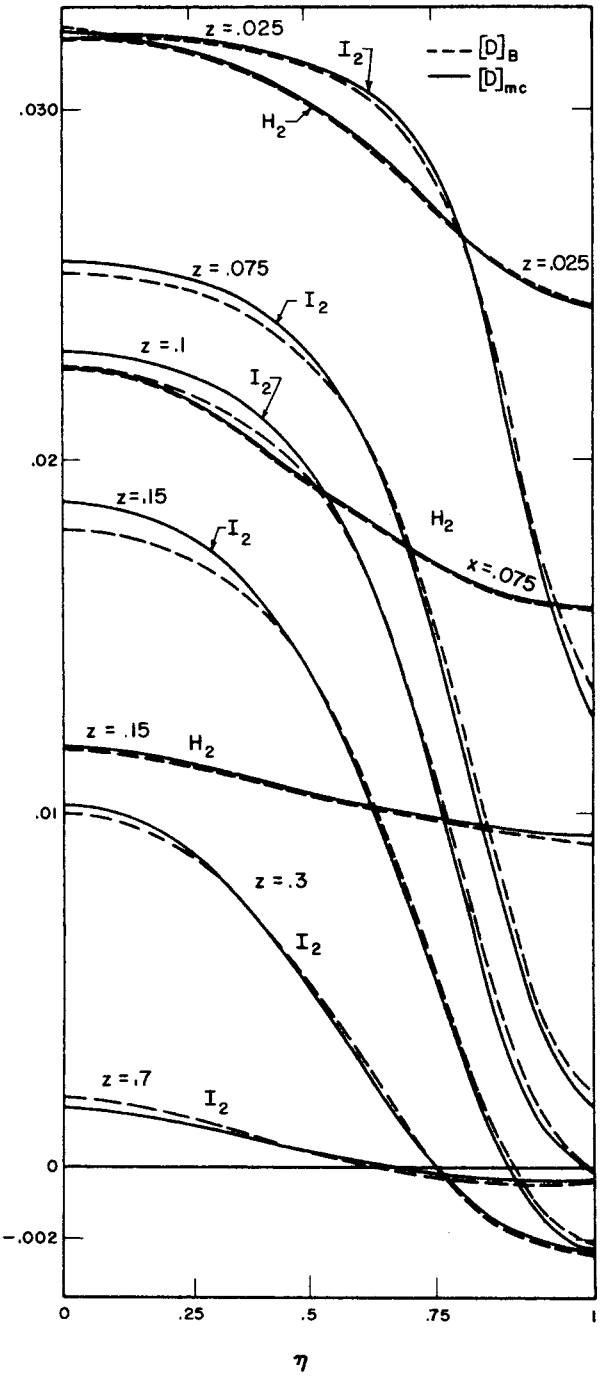

Fig. 2. Radial profiles of mole fraction in the tubular reactor near equilibrium; H_2, I_2; $P = 2.77$ atm., $T = 978°K.$; stoichiometric equilibrium ($H_2 + I_2 \rightleftarrows 2HI$).

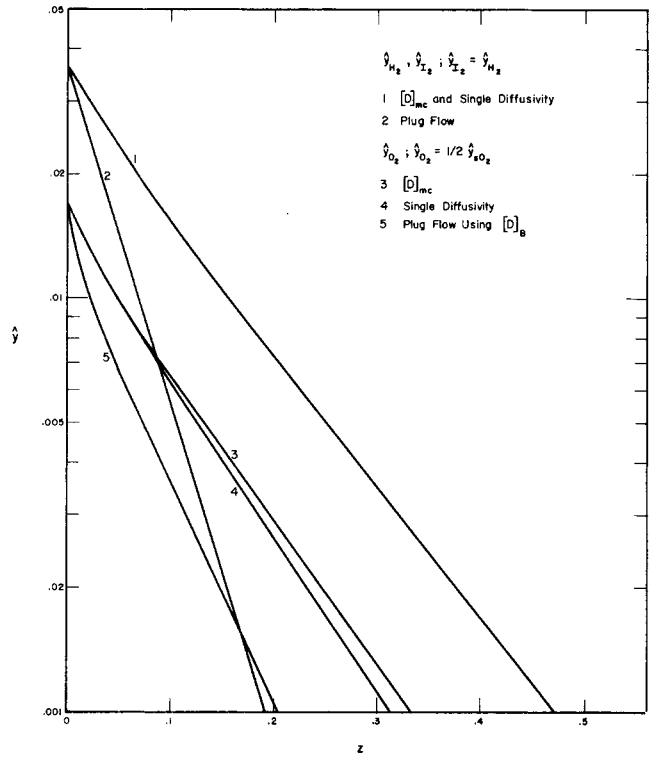

Fig. 3. Bulk mole fraction as function of axial position for the homogeneous reaction $H_2 + I_2 \rightleftarrows 2HI$ and the heterogeneous reaction $SO_2 + 1/2\ O_2 \rightleftarrows SO_3$.

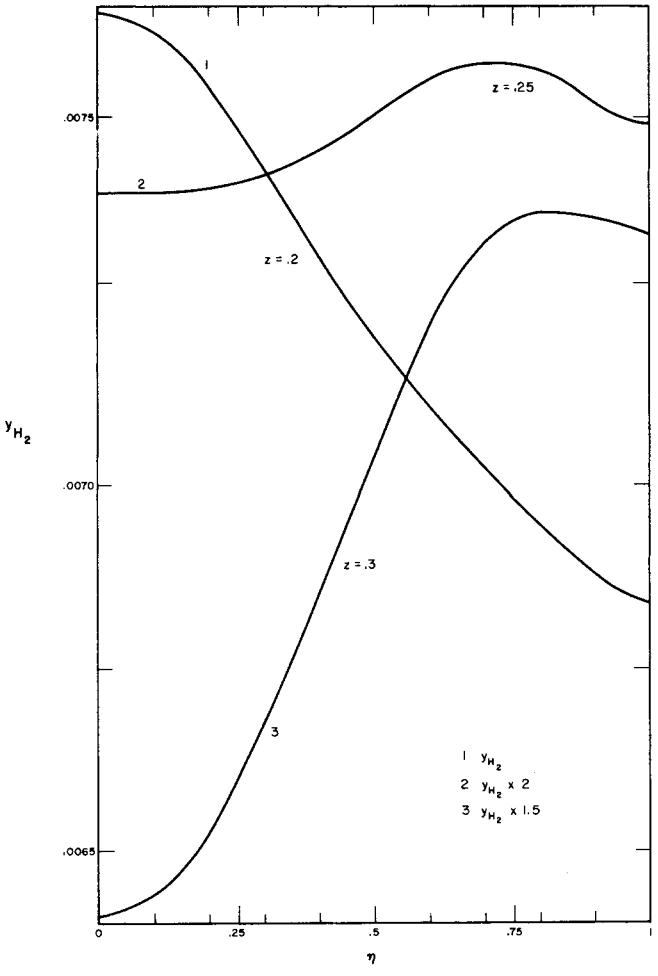

Fig. 4. Radial profile of H_2 mole fraction in the tubular reactor near equilibrium; $P = 2.77$ atm., $T = 978°K.$; stoichiometric equilibrium ($H_2 + I_2 \rightleftarrows 2HI$).

$$[D]_B = \begin{bmatrix} 1.0 & 0 \\ 0 & 0.0839 \end{bmatrix} \tag{28}$$

Components 1 and 2 are H_2 and I_2, respectively, where as usual the most concentrated component (here HI) has been eliminated. The reference diffusivity is given by $D_R = \mathcal{D}_{H_2,\,HI}$ at the temperature and pressure being considered. One of the off diagonal terms of $[D]_{MC}$ is large. Each element of the dimensionless rate constant matrix $[K]$ is -0.256. Since the equations are linear, the value of (y) at $z = 0$ is arbitrary. The values $y_1^0 = y_2^0 = 0.0365$ were chosen. (This lowers the HI mole fraction by 10% at the inlet.) Radial profiles of mole fraction are shown in Figure 1 for several axial distances. The solid and dotted curves were calculated using $[D]_{MC}$ and $[D]_B$, respectively. Despite the differences between (27) and (28) the profiles are almost the same; the cup-mixing mole fractions obtained with the two models are essentially identical. The I_2 radial gradient is large compared to that for H_2 since the former has lower diffusivities. The profiles always decrease with increasing radial position.

Consider now the effect of raising the pressure and thus of raising the dimensionless linearized rate constants, that is, $T = 978°K.$, $P = 2.77$ atm. The equilibrium mole fractions and the dimensionless diffusivity matrices are the same as above; the elements of the dimensionless rate constant matrix are increased to -2.43. The radial profiles of mole fraction are shown in Figure 2. Again the multicomponent and binary diffusivities predict approximately the same results. The cup-mixing mole fractions are shown in Figure 3 and those predicted using (27) and (28) are identical to the accuracy of the graph. For comparison the mole fraction distribution predicted using a plug-flow model is also shown; this was obtained analytically as shown in reference *24*. Returning to Figure 2 it is seen that as the fluid travels downstream the hydrogen profiles become very flat and the iodine profiles become rather steep because of the large difference in their diffusivities. The iodine mole fraction overshoots its equilibrium value in the wall region for $z \geq 0.10$; however, the hydrogen mole fraction always stays above its equilibrium value. The low iodine concentration near the wall causes a low rate of reaction there; the hydrogen profiles change from monotonically decreasing to monotonically increasing with increasing radial position as can be seen from Figure 4. Since the iodine overshoots its equilibrium value near the wall, the possibility exists that reaction reversal will take place; it can be shown from the reaction rate expression that this does occur farther downstream ($z = 0.7$). Thus HI is being formed near the tube center and decomposes near the tube wall. No overshoot occurs, however, in the cup-mixing mole fractions or in the averaged reaction rate. A pressure intermediate between that considered in Figure 1 and that considered in Figures 2, 3, and 4 was also treated, that is, $P = 1.96$ atm. Again the iodine overshoots its equilibrium value but in this case no reaction reversal occurs.

A somewhat higher pressure was also considered, namely, $P = 5.6$ atm., $T = 978°K.$ This is the highest pressure which can be treated, since the higher reaction rates require more terms in the series expansion. The radial profiles of the hydrogen mole fractions are shown in Figure 5. The curves shown were evaluated using $[D]_B$; similar results were obtained using $[D]_{MC}$. The change from monotonically decreasing to monotonically increasing dependence on radial position is again observed. However, in this case the hydrogen concentrations go past their equilibrium values near the tube center. The iodine profiles are not shown but resemble the results for $P = 2.77$ atm. shown in Figure 2.

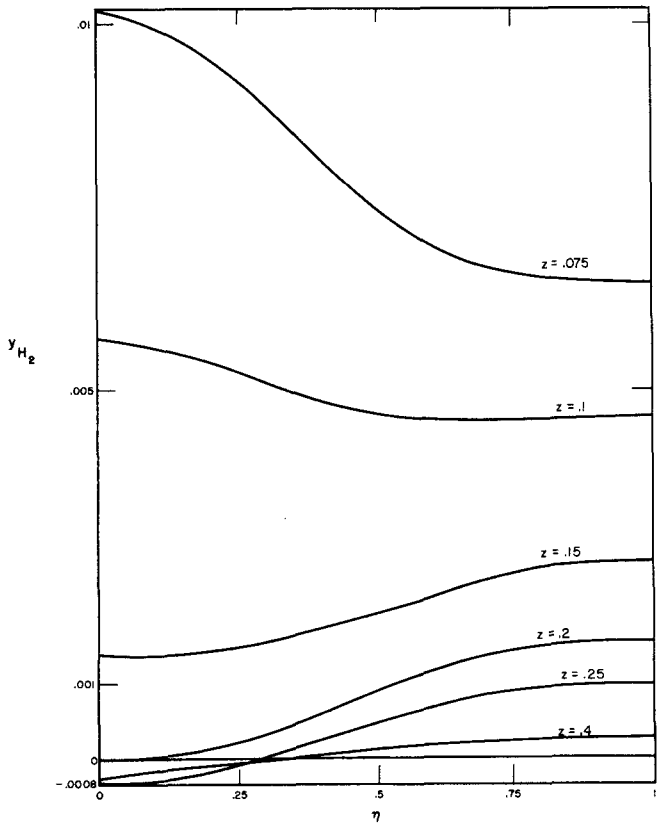

Fig. 5. Radial profile of H_2 mole fraction in the tubular reactor near equilibrium; $P = 5.6$ atm., $T = 978°K.$; stoichiometric equilibrium ($H_2 + I_2 \rightleftarrows 2HI$).

The closeness of the concentration profiles predicted using $[D]_{MC}$ and $[D]_B$ can be explained by considering (27) and (28). The only relatively large cross diffusivity involves the diffusional flux of iodine. The flux is $+0.133\ \nabla_\eta y_1 - 0.0951\ \nabla_\eta y_2$ for multicomponent diffusion and $-0.0839\ \nabla_\eta y_2$ for binary diffusion where the subscripts 1 and 2 denote hydrogen and iodine, respectively. In most of the reactor $|\nabla_\eta y_1| < |\nabla_\eta y_2|$ and both $\nabla_\eta y_1$ and $\nabla_\eta y_2$ are negative. The diffusional fluxes thus tend to be about the same. This is not true farther downstream where $\nabla_\eta y_1$ changes sign; however, most of the reaction has already taken place before this sign change.

The above calculations were repeated at a lower temperature, namely, $T = 781°K$. The results are qualitatively similar to those discussed above for $T = 978°K$.

The results predicted using $[D]_{MC}$ and $[D]_B$ are not always so similar. Consider for example a nonstoichiometric equilibrium composition rich in hydrogen, namely 51.06% H_2, 47.88% HI, and 1.06% I_2; $T = 794°K.$, $P = 10$ atm. Here hydrogen is eliminated from the equations so that the binary diffusivities of I_2 and of HI in H_2 are used in $[D]_B$. The diffusivity matrices are

$$[D]_{MC} = \begin{bmatrix} 0.208 & 0.022 \\ 1.001 & 1.209 \end{bmatrix}$$

$$[D]_B = \begin{bmatrix} 1.0 & 0 \\ 0 & 1.237 \end{bmatrix}$$

where component 1 is I_2 and 2 is HI. Some radial profiles of HI mole fraction are shown in Figure 6. For graphical convenience the inlet mole fraction difference y_{HI} was chosen to be positive. The deviation between the results predicted using $[D]_{MC}$ and $[D]_B$ is somewhat greater than that found above. No overshoot was predicted using either diffusivity matrix.

Calculations were also carried out for the gas phase reaction $CO + Cl_2 \rightleftarrows COCl_2$; details of the results can be found in reference *24*. In this case there is a volume change on reaction, which violates one of the assumptions made in the analysis. (The velocity profile is fully developed.) However it is shown (*24*) that the qualitative conclusions drawn from the study are correct. A range of reaction rate constants was covered, including very high reaction rates. No overshoot past equilibrium was found. The difference between this result and that obtained for the hydrogen iodide reaction can be explained by considering the diffusivities of the reacting species. The binary diffusivities $\mathcal{D}_{CO,\,COCl_2}$, $\mathcal{D}_{CO,\,Cl_2}$, and $\mathcal{D}_{Cl_2,\,COCl_2}$ are relatively close; the ratio of the largest to the smallest is approximately 3. The corresponding ratio for the hydrogen, iodine, and hydrogen iodide system is about 10. The multicomponent diffusion matrix for $COCl_2$ formation at 883°K., 30 atm., and an equal number of moles of Cl_2 and CO is

$$[D]_{MC} = \begin{bmatrix} 1.217 & -0.383 \\ -0.0802 & 1.905 \end{bmatrix} \qquad (29)$$

The diagonal diffusivities are close in magnitude, whereas in (27) they differ by about one order of magnitude. The results predicted using $[D]_B$ agreed very closely with those predicted using $[D]_{MC}$ for all the cases studied.

The surface reaction $SO_2 + \frac{1}{2}\ O_2 \rightleftarrows SO_3$ was also considered. At temperatures less than 700°K., which are the conditions used industrially, the reaction goes to completion. Since conditions near equilibrium are being treated

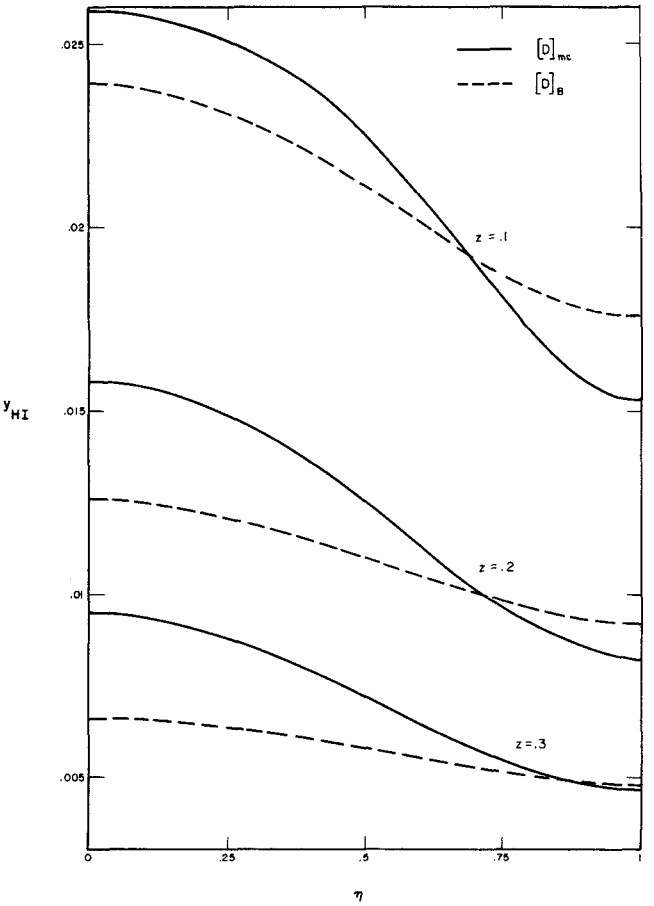

Fig. 6. Radial profile of HI mole fraction in the tubular reactor near equilibrium; $P = 10$ atm., $T = 794°K.$; equilibrium mole fractions $x_{H_2} = 0.5106$, $x_{HI} = 0.4788$, $x_{I_2} = 0.0106$ ($H_2 + I_2 \rightleftarrows 2HI$).

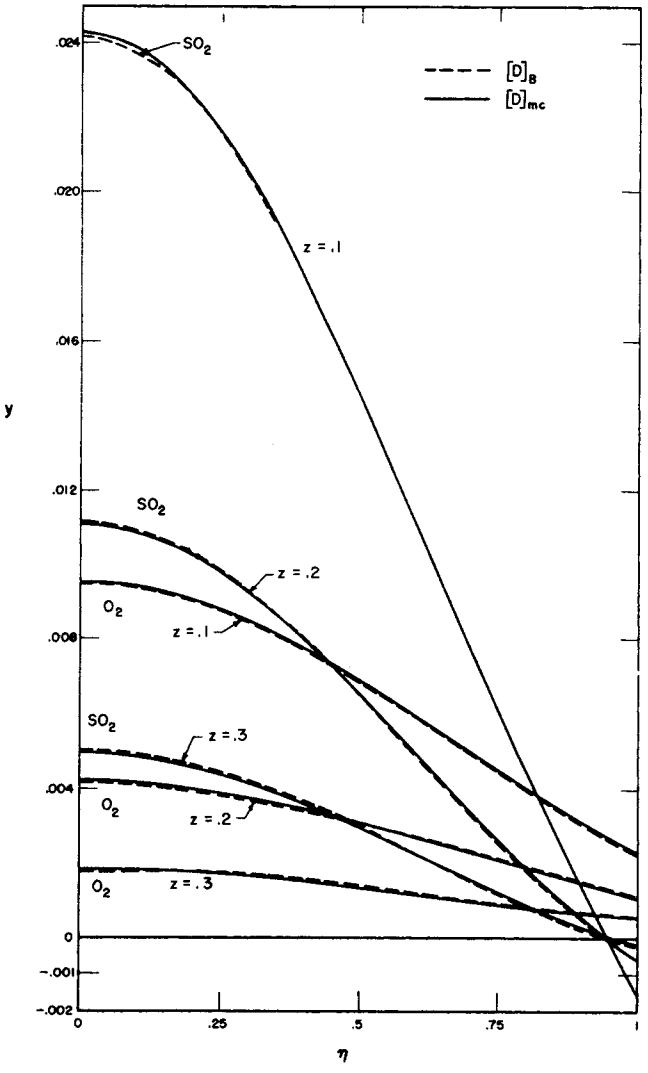

Fig. 7. Radial profiles of mole fraction in the tubular reactor near equilibrium; O_2, SO_2; $P = 1.0$ atm., $T = 955°K.$; stoichiometric equilibrium ($SO_2 + 1/2\ O_2 \rightleftharpoons SO_3$).

in this work, temperatures greater than 900°K. are considered where there is a significant concentration of SO_2 and O_2 at equilibrium. At $T = 955°K.$, $P = 1$ atm., and stoichiometric amounts of SO_2 and O_2, the equilibrium is 35% SO_2, 17.5% O_2, and 47.5% SO_3 on a molar basis. The elements of the first row of the dimensionless linearized surface rate matrix $[F]$ are 28.24 and the elements of the second row are 14.17. Component 1 is SO_2, component 2 is O_2, and the most concentrated component SO_3 has been eliminated. The tube radius was chosen to be 0.5 cm. The diffusivity matrices are

$$[D]_{MC} = \begin{bmatrix} 1.10 & -0.34 \\ -0.03 & 1.77 \end{bmatrix} \tag{30}$$

and

$$[D]_B = \begin{bmatrix} 1.0 & 0 \\ 0 & 1.76 \end{bmatrix} \tag{31}$$

At the inlet to the reactor the mole fractions of O_2 and SO_2 were increased 10%. Radial profiles of mole fraction are shown in Figure 7. The multicomponent and binary diffusivities predict essentially the same results. The SO_2 overshoots its equilibrium value near the wall. It should be noted that this overshoot did not occur for the gas-phase phosgene reaction even though the diffusivity matrix (29) is very similar to (30). For a gas-phase reaction the difference in the diagonal diffusivities has to be much larger for overshoot to occur, for example see (27) for the hydrogen iodide reaction. If the temperature is decreased to 902°K. for the SO_3 formation, the rate matrix is reduced to about one-third its value at 955°K. and the dimensionless diffusivity matrices remain about the same. In this latter case the overshoot of the SO_3 concentration past equilibrium is very slight; at lower temperatures the overshoot will not occur. The cup-mixing mole fractions for O_2 and SO_2 are shown in Figure 3. If the parabolic velocity profile is replaced by plug flow and $[D]_B$ is used, the problem can be solved analytically; this analytical solution is presented in reference *24* and the result is shown in Figure 3 for comparison.

In all of the above cases the calculated eigenvalues are real. Thus, although overshoots occur, no oscillations of concentrations can occur with increasing axial position. This is due to the fact that the systems were always held near equilibrium. This is consistent with previous findings of Bak (*1*), Prigogine (*20*), and Toor (*31*). A discussion is presented in reference *26* on the meaning of "near equilibrium."

Many of the above calculations were repeated using the diffusivity matrix $[D]_E$ where the diagonal elements are defined by (7) and the off diagonal terms are zero. In general, the results compared poorly with those predicted using $[D]_{MC}$ (*24*).

The use of either $[D]_B$ or $[D]_E$ rather than the multicomponent diffusivity matrix $[D]_{MC}$ offers no mathematical simplification in the solution of Equations (3). The equations given by (3) cannot be uncoupled when any of these three diffusivity matrices is used. Any transformation which diagonalizes the reaction matrix leaves the equations coupled through the diffusion. This has been discussed in detail by Toor (*31*). However, if the diffusivity matrix is a constant times the identity matrix, that is, $\bar{D}[I]$ and either $[K]$ or $[F]$ is zero, uncoupling is possible and the governing equations can be solved separately. Because of the great mathematical simplification, it is of interest to determine if a single diffusivity can be found which when used in Equations (3) can duplicate the results predicted using the multicomponent diffusivity matrix $[D]_{MC}$. Such a single diffusivity cannot duplicate the radial mole fraction profiles given above. The single diffusivity would predict that the mole fractions of the reactants would be everywhere stoichiometric; for example, in Figures 1 and 2 the hydrogen and iodine profiles would be identical. However, the cup-mixing mole fractions shown in Figure 3 could be duplicated. Several methods of finding $\bar{D} = \bar{D}^*/D_R$ were tried. For example, taking $\bar{D}^*$ as the average of the three binary diffusivities was tried and was found to give poor results. The method which yields consistently good results in predicting cup-mixing mole fractions is a modification of the Wilke-Lee formula (*19*, *33*). The most concentrated component at equilibrium is designated as 3. Average values of the parameters are calculated for components 1 and 2. These averages are then combined with the properties of 3 in the Wilke-Lee formulas to calculate $\bar{D}^*$. The average molecular weight is given by

$$M_A = \left\{ \frac{x_1}{1 - x_3} \right\}_e M_1 + \left\{ \frac{x_2}{1 - x_3} \right\}_e M_2$$

The average force constant and collision diameter are

$$\{\epsilon/k\}_A = [\{\epsilon/k\}_1 \{\epsilon/k\}_2]^{1/2}$$

$$r_A = \frac{r_1 + r_2}{2}$$

Then $\bar{D}^*$ is given by

$$\overline{D}^{\,*} = \frac{\left[10.7 - 2.46\left\{\frac{1}{M_A} + \frac{1}{M_3}\right\}^{1/2}\right] 10^{-4}\, T^{3/2}\left[\frac{1}{M_A} + \frac{1}{M_3}\right]^{1/2}}{P\, r_{A3}^{\,2}\, f\left\{\left\{\frac{kT}{\epsilon}\right\}_{A3}\right\}} \qquad (32)$$

where

$$r_{A3} = \frac{r_A + r_3}{2}$$

$$\left\{\frac{\epsilon}{k}\right\}_{A3} = \left[\left\{\frac{\epsilon}{k}\right\}_A \left\{\frac{\epsilon}{k}\right\}_3\right]^{1/2}$$

and f is the tabulated collision integral (*19*). The cup-mixing mole fractions were found using the single dimensionless diffusivity $\overline{D} = \overline{D}^{\,*}/D_R$. The results compared very well with those predicted using $[D]_{MC}$. Representative results are shown in Figure 3. For the hydrogen iodide reaction, the results using $\overline{D}$ and $[D]_{MC}$ are identical to the accuracy of the graph. For the surface reaction the results predicted using $\overline{D}$ are somewhat below those predicted using $[D]_{MC}$.

NOTATION

a_{ij} = expansion coefficient as defined by Equation (14)
$[A]$ = matrix as defined by Equation (19)
$[B]$ = matrix as defined by Equation (19)
c = molar concentration, mole/cu.cm.
$[C]$ = matrix of eigenvectors
D_R = reference diffusivity, sq.cm./sec.
$\overline{D}^{\,*}$ = single effective diffusivity as defined by Equation (32), sq.cm./sec.
$\mathcal{D}_{ij}$ = binary diffusivity, sq.cm./sec.
$[D]$ = $[D^*]/D_R$, diffusivity matrix, dimensionless
$[D^*]$ = diffusivity matrix, sq.cm./sec.
$[D]_B$ = binary diffusivity matrix, dimensionless
$[D]_E$ = effective diffusivity matrix, dimensionless
$[D]_{MC}$ = multicomponent diffusivity matrix, dimensionless
$[F]$ = $[F^*]R/D_R$
$[F^*]$ = surface reaction rate matrix, cm./sec.
$[H]$ = matrix as defined by Equation (13*a*)
$[I]$ = identity matrix
J_i^* = molar flux, mole/(sq.cm.)(sec.)
k = Boltzman's constant
$[K]$ = $[K^*]R^2/D_R$
$[K^*]$ = gas-phase reaction rate matrix, sec.$^{-1}$
$[L]$ = matrix as defined by Equation (13*b*)
M = number of terms in series expansion
M_i = molecular weight of i^{th} component
M_A = average molecular weight
P = pressure, atm.
$[P]$ = matrix as defined by Equation (24)
(Q) = vector as defined by Equation (23)
r_1 = collision diameter for component 1
R = tube radius, cm.
T = temperature, °K.
$[T]$ = modal matrix of $[D]^{-1}[F]$
V = fluid velocity at axis, cm./sec.
$[W]$ = $[A] + [B]$
(x) = mole fraction vector
$(x)_e$ = mole fraction vector at equilibrium
(y) = $(x) - (x)_e$
$(y)^0$ = value of (y) at $z = 0$
$(\hat{y})$ = cup mixing mole fraction
z = z^*D_R/VR
z^* = axial position, cm.
$[Z]$ = matrix as defined by Equations (17) and (18)

Greek Letters

α_{ij} = root of Equation (15)
η = radial position, dimensionless, scaled using tube radius
λ_i = eigenvalue
$[\mu]$ = matrix as defined by Equation (10)
(ψ) = $[T]^{-1}(y)$
ω_i = expansion coefficient, Equation (10)

Subscripts

A = averaged property of components 1 and 2
e = equilibrium

LITERATURE CITED

1. Bak, Thor A., "Contributions to the Theory of Chemical Kinetics," W. A. Benjamin, New York (1963).
2. Baron, Thomas, W. R. Manning, and H. F. Johnstone, *Chem. Eng. Progr.*, **48**, 125 (1952).
3. Bird, R. Byron, Warren E. Stewart, and Edwin N. Lightfoot, "Transport Phenomena," Wiley, New York (1962).
4. Bodenstein, Max, *Z. Phys. Chem.*, **29**, 295 (1899).
5. Burchard, John K., and H. L. Toor, *J. Phys. Chem.*, **66**, 2015 (1962).
6. Cullinan, Harry T., Jr., *Ind. Eng. Chem. Fundamentals*, **4**, 133 (1965).
7. Cussler, E. L., Jr., and E. N. Lightfoot, *AIChE J.*, **9**, 783 (1963).
8. Graven, Wendell M., *J. Am. Chem. Soc.*, **78**, 3297 (1956).
9. Hirschfelder, Joseph O., Charles F. Curtis, and R. Byron Bird, "Molecular Theory of Liquids and Gases," Wiley, New York (1954).
10. Hsu, Chia-Jung, *AIChE J.*, **11**, 938 (1965).
11. Hudson, J. L., *ibid.*, **11**, 943 (1965).
12. *Ibid.*, **13**, 961 (1967).
13. Katz, S., *Chem. Eng. Sci.*, **10**, 202 (1959).
14. Lauwerier, H. A., *Appl. Sci. Res.* **A8**, 366 (1959).
15. Lyczkowski, R. W., Dimitri Gidaspow, and C. W. Solbrig, *Inst. Gas Technol. Rept. Basic Res. Proj.* (1968).
16. Pao, Yih-Ho, *Chem. Eng. Sci.*, **19**, 694 (1964).
17. *Ibid.*, **20**, 665 (1965).
18. Parlett, Beresford, *Math. Comp.*, **18**, 464 (1964).
19. Perry, Robert H., Cecil H. Chilton, and Sidney D. Kirkpatrick, ed., "Chemical Engineers Handbook," 4th edit., McGraw-Hill, New York (1963).
20. Prigogine, I., "Introduction to the Thermodynamics of Irreversible Processes," 3rd edit., Interscience, New York (1967).
21. Solbrig, Charles W., and Dimitri Gidaspow, *Can. J. Chem. Eng.*, **45**, 35 (1967).
22. ———, *AIChE J.*, **13**, 346 (1967).
23. Solomon, Robert Lee, M.S. thesis, Univ. Illinois, Urbana (1967).
24. ———, Ph.D. thesis, Univ. Illinois, Urbana (1969).
25. ———, and J. L. Hudson, *AIChE J.*, **13**, 545 (1967).
26. ———, and ———, *ibid.*, **17**, 379 (1971).
27. Stewart, Warren E., and Richard Prober, *Ind. Eng. Chem. Fundamentals*, **3**, 224 (1964).
28. Sullivan, John H., *J. Chem. Phys.*, **46**, 73 (1967).
29. Toor, H. L., *AIChE J.*, **10**, 448 (1964).
30. *Ibid.*, **10**, 460 (1964).
31. ———, *Chem. Eng. Sci.*, **20**, 941 (1965).
32. Vignes, J. P., and P. J. Trambouze, *Chem. Eng. Sci.*, **17**, 73 (1962).
33. Wilke, C. R., and C. Y. Lee, *Ind. Eng. Chem*, **47**, 1253 (1955).
34. Wissler, E. H., and R. S. Schechter, *Appl. Sci. Res.*, **A10**, 198 (1961).

Manuscript received April 24 1969; revision received February 24, 1970, paper accepted March 2, 1970.